

## Effect of the Vortices on the Nuclear Spin Relaxation Rate in the Unconventional Pairing States of the Organic Superconductor $(\text{TMTSF})_2\text{PF}_6$

M. Takigawa,<sup>1,\*</sup> M. Ichioka,<sup>2</sup> K. Kuroki,<sup>3</sup> Y. Asano,<sup>1</sup> and Y. Tanaka<sup>4</sup>

<sup>1</sup>*Department of Applied Physics, Hokkaido University, Sapporo 060-8628, Japan*

<sup>2</sup>*Department of Physics, Okayama University, Okayama 700-8530, Japan*

<sup>3</sup>*Department of Applied Physics and Chemistry, The University of Electro-Communications, Chofu, Tokyo 182-8585, Japan*

<sup>4</sup>*Department of Material Science and Technology, Nagoya University, Nagoya 464-8603, Japan*

(Received 10 January 2006; published 3 November 2006)

This Letter theoretically discusses quasiparticle states and nuclear spin relaxation rates  $T_1^{-1}$  in the quasi-one-dimensional superconductor  $(\text{TMTSF})_2\text{PF}_6$  under a magnetic field applied parallel to the conduction chains. We study the effects of Josephson-type vortices on  $T_1^{-1}$  by solving the Bogoliubov–de Gennes equation for  $p$ -,  $d$ - or  $f$ -wave pairing interactions. In the presence of line nodes in pairing functions,  $T_1^{-1}$  is proportional to  $T$  in sufficiently low temperatures because quasiparticles induced by vortices at the Fermi energy relax spins. We also try to identify the pairing symmetry of  $(\text{TMTSF})_2\text{PF}_6$ .

DOI: [10.1103/PhysRevLett.97.187002](https://doi.org/10.1103/PhysRevLett.97.187002)

PACS numbers: 74.70.Kn, 74.20.Rp, 74.25.Op, 76.60.-k

Recently, much attention has been focused on superconductivity in a Bechgaard salt  $(\text{TMTSF})_2\text{PF}_6$  [1], where a superconducting phase appears next to a spin density wave phase in the pressure-temperature phase diagram [2]. So far a number of theories have proposed unconventional superconductivity in this quasi-one-dimensional (Q1D) organic superconductor: spin-singlet  $d$ -wave [3–6], triplet  $p$ -wave [7–9], and triplet  $f$ -wave symmetries [10–15]. Although pairing interaction along the chain direction is a common conclusion among these theories, the pairing symmetry itself has been controversial. Experimentally, the spin-triplet pairing has been suggested from the unchanged Knight shift across the superconducting transition temperature  $T_c$  in the NMR experiment [16] and the large enhancement of  $H_{c2}$  exceeding the Pauli limit [17]. The nuclear spin relaxation experiment is a powerful tool to identify the orbital part of the pairing function. The relaxation rate  $T_1^{-1}$  should exhibit an exponential temperature ( $T$ ) dependence for fully gapped superconductors, while it is proportional to  $T^3$  in the presence of line nodes in the gap. Such a theoretical analysis was applied to the TMTSF salts by Hasegawa and Fukuyama [18]. In  $(\text{TMTSF})_2\text{ClO}_4$ , the relation  $T_1^{-1} \propto T^3$  as well as the absence of the coherence peak were observed at zero magnetic field, which indicates the presence of line nodes [19]. In  $(\text{TMTSF})_2\text{PF}_6$ , however, Lee *et al.* [16] observed  $T_1^{-1} \propto T$  in low temperatures under a magnetic field at 1.43 T. Under a magnetic field, quasiparticles induced at the Fermi energy may cause the spin relaxation. In fact, two of the present authors and other groups have shown that the relation  $T_1^{-1} \propto T$  holds in a number of nodal superconductors [20–23]. In the NMR experiment by Lee *et al.* [16], however, the magnetic field is applied parallel to the conduction chains. At first sight, this experimental configuration seems to remove such quasiparticle contributions from  $T_1^{-1}$  because the order parameter is mainly localized around the chain, and the

vortices pass through the open space between the chains. Thus order parameters along the chain are expected to be unchanged from their value at the zero magnetic field [24–26]. However, no theoretical study has ever tried to reveal effects of such Josephson vortices on quasiparticle states and  $T_1^{-1}$ .

There are two main purposes to this Letter: (i) studying temperature dependences of  $T_1^{-1}$  in the Q1D organic superconductor in the presence of vortices, and (ii) identifying the pairing symmetry of  $(\text{TMTSF})_2\text{PF}_6$ . For these purposes, we calculate quasiparticle states and order parameters self-consistently in the presence of the magnetic field along the chain direction based on the Bogoliubov–de Gennes (BdG) equation. Three pairing symmetries (i.e.,  $p$ ,  $d$ , and  $f$  waves) are assumed on a tight-binding lattice. We will show that the relation  $T_1^{-1} \propto T$  holds at low temperatures for  $d$ - and  $f$ -wave symmetries.

We consider a three-dimensional tight-binding model, where the transfer integrals between the nearest neighbor sites are  $-t_a$ ,  $-t_b$ , and  $-t_c$  in the  $a$ ,  $b$ , and  $c$  directions, respectively. The band dispersion is given by  $E(\mathbf{k}) = -2t_a \cos k_a - 2t_b \cos k_b - 2t_c \cos k_c - \mu$ . To describe the electronic structure of  $(\text{TMTSF})_2\text{PF}_6$ , we set  $t_a:t_b:t_c = 10:1:0.03$  and tune the chemical potential  $\mu$  to keep the band filling at quarter filling (i.e.,  $\langle n \rangle = 0.5$ ). The Q1D Fermi surface for these parameters is shown in Fig. 1(a). We introduce a spin-singlet pairing interaction between the second nearest neighbor sites in the chain direction ( $a$  axis) in the case of the  $d$ -wave symmetry [27]. For the  $p$ -wave ( $f$ -wave) pairing symmetry, we introduce a spin-triplet pairing interaction [28] between the second (fourth) nearest sites in the  $a$  direction. The pairing functions result in  $\psi(k_a) = \cos 2k_a$ ,  $\sin 2k_a$ , and  $\sin 4k_a$  for the  $d$ -,  $p$ -, and  $f$ -wave pairings, respectively. By applying the Fourier transformation in the  $a$  axis, the Hamiltonian is given by

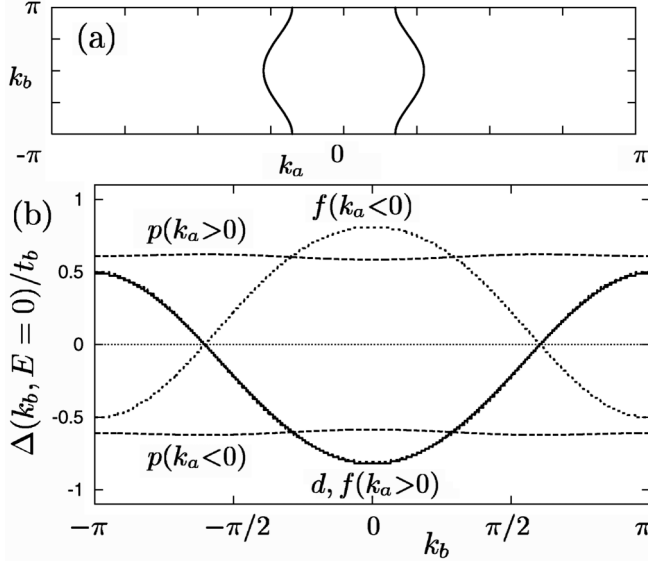


FIG. 1. (a) Fermi surface in the Q1D tight-binding model [ $E(\mathbf{k}) = 0$ ] in the  $k_a$ - $k_b$  plane.  $k_c$  dependence of the Fermi surface is negligible in this scale of the figure. (b) The gap function  $\Delta_0 \psi(k_a)$  along the Fermi surface for  $p$ -,  $d$ -, and  $f$ -wave pairing symmetries at  $T = 0$  and  $H = 0$ .

$$\mathcal{H} = \sum_{k_a, j, i, \sigma} K_{k_a, i, j} a_{j, \sigma}^\dagger a_{i, \sigma} + \sum_{k_a, i} \{ \Delta_i^\dagger \psi(k_a) a_{i, \downarrow} a_{i, \uparrow} + \Delta_i \psi(k_a) a_{i, \uparrow}^\dagger a_{i, \downarrow}^\dagger \}, \quad (1)$$

where  $K_{k_a, i, j} = -\tilde{t}_{i, j} + \delta_{i, j}(-2t_a \cos k_a - \mu)$ ,  $a_{i, \sigma}^\dagger$  ( $a_{i, \sigma}$ ) is a creation (annihilation) operator of an electron with spin  $\sigma$  ( $=\uparrow$  or  $\downarrow$ ), and  $i = (i_b, i_c)$  is a site index in the  $bc$  plane. For a magnetic field applied along the  $a$  direction [ $\mathbf{H} = (H, 0, 0)$ ], the transfer integral in the  $bc$  plane becomes  $\tilde{t}_{i, j} = t_{i, j} \exp[i \frac{\pi}{\phi_0} \int_{\mathbf{r}_i}^{\mathbf{r}_j} \mathbf{A}(\mathbf{r}) \cdot d\mathbf{r}]$ , where  $\phi_0$  is the flux quantum and the vector potential is taken to be  $\mathbf{A}(\mathbf{r}) = \frac{1}{2} \mathbf{H} \times \mathbf{r}$  in the symmetric gauge.

From Eq. (1), the BdG equation is derived for each  $k_a$ :

$$\sum_i \begin{pmatrix} K_{k_a, i, j} & D_{k_a, i, j} \\ D_{k_a, i, j}^\dagger & -K_{k_a, i, j}^* \end{pmatrix} \begin{pmatrix} u_{\epsilon, j} \\ v_{\epsilon, j} \end{pmatrix} = E_\epsilon \begin{pmatrix} u_{\epsilon, i} \\ v_{\epsilon, i} \end{pmatrix}, \quad (2)$$

where  $u_{\epsilon, i}$  and  $v_{\epsilon, i}$  are the wave functions belonging to the eigenvalue  $E_\epsilon$ , and  $D_{k_a, i, j} = \psi(k_a) \Delta_i \delta_{i, j}$ . The self-consistent equation for the pair potentials is given by

$$\Delta_i = U \sum_\epsilon u_{\epsilon, i} v_{\epsilon, i}^* \psi(k_a) f(E_\epsilon), \quad (3)$$

where  $f(E)$  is the Fermi distribution function and  $U$  is the strength of the pairing interaction.

We consider that two vortices accommodate in a unit cell of  $20 \times 6$  lattice sites in the  $bc$  plane and form a triangular lattice. Note that the coherence length becomes anisotropic in the  $bc$  plane (i.e.,  $\xi_b \cdot \xi_c \propto t_b^{1/2} \cdot t_c^{1/2}$ ). By introducing the quasimomentum of the magnetic Bloch

state, the wave functions are calculated for sufficient quantities of unit cells connected by the periodic boundary condition [20]. We iterate the calculation of Eqs. (2) and (3) alternately until a self-consistent solution is obtained. Using the self-consistent solution ( $u_{\epsilon, i}$ ,  $v_{\epsilon, i}$ , and  $E_\epsilon$ ), the local density of states (LDOS) is given by

$$N(E, \mathbf{r}_i) = \sum_\epsilon \{ |u_{\epsilon, i}|^2 \delta(E - E_\epsilon) + |v_{\epsilon, i}|^2 \delta(E + E_\epsilon) \}. \quad (4)$$

The screening current  $\mathbf{J}(\mathbf{r})$  is also calculated. For instance, the current component in the  $b$  direction is given by  $J_b(\mathbf{r}_i) \propto \text{Im}[\tilde{t}_{i, i+\hat{b}} \sum_\epsilon \{ u_{\epsilon, i} u_{\epsilon, i+\hat{b}}^* f(E_\epsilon) + v_{\epsilon, i}^* v_{\epsilon, i+\hat{b}} [1 - f(E_\epsilon)] \}]$ , where  $i + \hat{b}$  denotes the nearest neighbor site to  $i$  in the  $b$  direction [20]. In the calculation, we take  $U = -38t_b$  (giving  $\Delta_0 = 2.4t_b$  and  $T_c = 1.05t_b$ ) for  $d$ -wave pairing,  $U = -15t_b$  ( $\Delta_0 = 0.62t_b$  and  $T_c = 0.35t_b$ ) for  $p$ -wave pairing, and  $U = -27.5t_b$  ( $\Delta_0 = 1.3t_b$  and  $T_c = 0.55t_b$ ) for  $f$ -wave pairing with  $\Delta_0 = \Delta_i (H = 0)$ . Here  $U$  is changed depending on pairing symmetries so that we have similar gap values in the three symmetries. The ratio  $\Delta_0/T_c$  depends on the anisotropy of  $|\psi(k_a)|$ . Figure 1(b) shows the superconducting gap  $\Delta_0 \psi(k_a)$  along the Fermi surface at  $H = 0$  for each symmetry.

First, we briefly summarize the density of states (DOS) spectra  $N(E, \mathbf{r}_i)$  in the absence of the magnetic field (i.e., in the uniform state) as shown by the dashed lines in Fig. 2. The dotted lines in Fig. 2 denote the DOS in the normal state. In the  $p$ -wave symmetry, no nodes exist in the gap along the Fermi surface as shown in Fig. 1(b). Correspondingly, the full gap structure can be seen in the DOS as shown in Fig. 2(a). Two peaks at  $E = \pm 0.65t_b$  reflect the large enhancement of the DOS at the gap edge. In the  $d$ - and  $f$ -wave symmetries, the gap functions have line nodes at  $k_a = \pm \pi/4$  on the Fermi surface. As a result, the DOS shows a V-shaped gap structure at  $H = 0$  (i.e.,  $E$ -linear DOS at low energies) as shown by the dashed lines in Figs. 2(b) and 2(c).

Before turning to the DOS in the presence of vortices, a typical spatial profile of the pair amplitude under the magnetic field should be discussed. In Fig. 3(a), we show

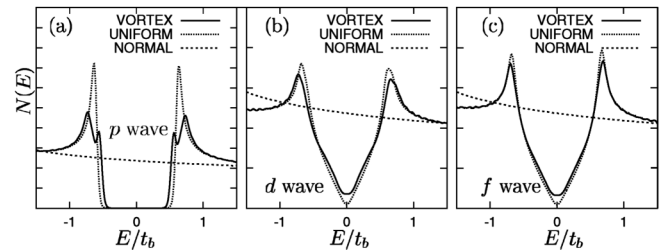


FIG. 2. The LDOS  $N(E, \mathbf{r})$  at the site nearest to the vortex core is presented at  $T = 0$  for the  $p$  wave in (a), the  $d$  wave in (b), and the  $f$  wave in (c). The LDOS in the vortex state is plotted with solid lines. The results in the uniform state at zero field and those in the normal state are shown with the dashed and dotted lines, respectively.

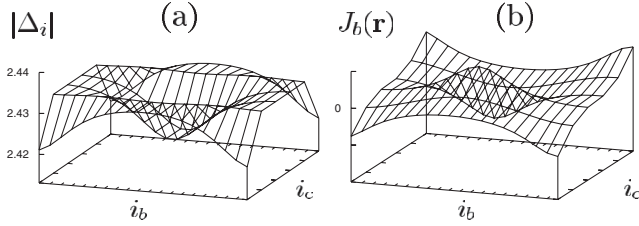


FIG. 3. Spatial profiles of the pair amplitudes and supercurrents in a unit cell are shown for the  $d$ -wave symmetry at  $T = 0$ . In (a), the amplitudes of the pair potentials ( $|\Delta_i|$ ) are presented. In (b), the amplitudes of the  $b$  component of the screening current [ $J_b(\mathbf{r})$ ] are presented.

$|\Delta_i|$  for the  $d$ -wave symmetry for instance. Since the vortex center is located in the space between conduction chains,  $|\Delta_i|$  is suppressed very slightly even near the vortex. The screening current flows around the vortex as shown in Fig. 3(b), where the  $b$  component of the supercurrent is presented. Compared to the conventional vortex structure, the screening current flows in much wider region around the vortex. These features are typical characters of the Josephson vortex in layered superconductors [24–26].

Second, we show the LDOS in the vortex state as presented by the solid lines in Fig. 2, where we show  $N(E, \mathbf{r})$  at the lattice site nearest to the vortex. In the fully gapped  $p$ -wave symmetry, quasiparticles have bound states around the Josephson-type vortex with the energy near the full gap energy [25]. The two smaller peaks in LDOS around  $E \sim \pm 0.56t_b$  reflect such bound states. The larger peaks around  $E \sim \pm 0.73t_b$  correspond to gap edges smeared by the magnetic field. In the  $p$  wave, there is no quasiparticle states at the Fermi energy and the wide gap remains even in the presence of vortices. Such behaviors are typically found in the quasiparticle states around the Josephson vortex in full gap superconductors. In the  $d$ -wave [Fig. 2(b)] and  $f$ -wave [Fig. 2(c)] symmetries, on the other hand, the V-shaped superconducting gap is filled with low energy quasiparticles induced by vortices. Although suppression of  $\Delta_i$  around the Josephson vortex

is very small as shown in Fig. 3(a), vortices surely induce quasiparticles at the Fermi energy. Quasiparticles cannot form a zero-energy peak of the vortex core state because of the small suppression of  $\Delta_i$  [20,21]. In both the  $d$  and  $f$  waves, there are no bound states of quasiparticle in vortices because of line nodes. The calculated results in Fig. 2 show characteristic low energy quasiparticle excitations depending on the gap functions under the magnetic field.

Next we discuss the  $T$  dependence of  $T_1^{-1}$  on the basis of the calculated results in Fig. 2. The spin-spin correlation function  $\chi_{\pm}(\mathbf{r}_i, \mathbf{r}_{i'}, i\Omega_n)$  can be calculated from the wave functions of the BdG equation. The nuclear spin relaxation rate is given by [20,21]

$$R(\mathbf{r}_i, \mathbf{r}_{i'}) = \text{Im} \chi_{+,-}(\mathbf{r}_i, \mathbf{r}_{i'}, i\Omega_n \rightarrow \Omega + i\eta) / (\Omega/T) |_{\Omega \rightarrow 0} \\ = - \sum_{\epsilon, \epsilon'} [u_{\epsilon, i} u_{\epsilon', i'}^* v_{\epsilon, i} v_{\epsilon', i'}^* \\ - v_{\epsilon, i} u_{\epsilon', i'}^* u_{\epsilon, i} v_{\epsilon', i'}^*] \pi T f'(E_{\epsilon}) \delta(E_{\epsilon} - E_{\epsilon'}). \quad (5)$$

We choose  $\mathbf{r}_i = \mathbf{r}_{i'}$  because the nuclear spin relaxation at a local lattice site is dominant. A relation  $\delta(x) = \pi^{-1} \text{Im}(x - i\eta)$  is used to handle the discrete energy levels of the finite size calculation. We typically use  $\eta = 0.02t_b$ . In Fig. 4, we show  $T_1^{-1}$  as a function of  $T$  at the lattice site nearest to the vortex core with solid lines. Although the relaxation time defined by  $T_1(\mathbf{r}) = 1/R(\mathbf{r}, \mathbf{r})$  depends on  $\mathbf{r}$ , results in the following are almost independent of  $\mathbf{r}$ . In the normal state, we reproduce the  $T$ -linear behavior of the Korringa law as shown by the dotted lines in Fig. 4. In the  $p$  wave [Fig. 4(a)],  $T_1^{-1}$  shows an exponential  $T$  dependence for both the vortex and uniform states. Effects of the vortices on  $T_1^{-1}$  are almost negligible in low temperatures because there are no quasiparticle states around the Fermi energy even in the presence of magnetic field as shown in Fig. 2(a). By contrast, in the  $d$ -wave symmetry in Fig. 4(b) and the  $f$ -wave symmetry in Fig. 4(c),  $T_1^{-1}$  deviates from  $T^3$  behavior and becomes proportional to  $T$  at low temperatures as observed in the experiment [16] (see the double logarithmic chart in the insets). This implies that

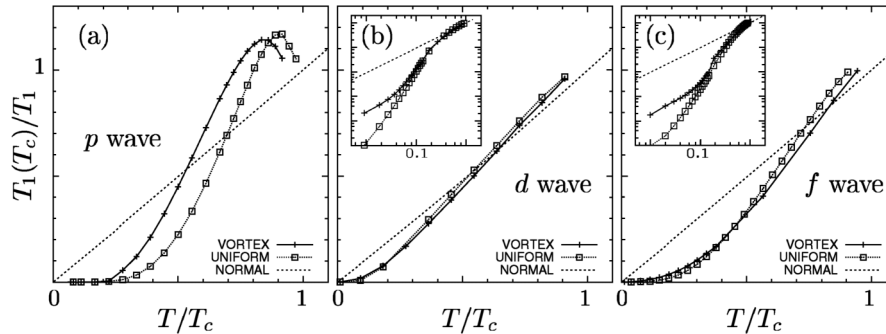


FIG. 4. The nuclear spin relaxation rate  $T_1^{-1}$  is shown as a function of temperature for (a)  $p$ -wave, (b)  $d$ -wave, and (c)  $f$ -wave symmetries. Solid lines denote  $T_1^{-1}$  at the lattice site nearest to the vortex core. The results for the uniform state at  $H = 0$  and those in the normal state are plotted with dashed and dotted lines, respectively. Insets in (b) and (c) show the double logarithmic chart of the results.

the quasiparticles at the zero-energy relax spins as they do in the normal state. Although the temperature at which  $T_1^{-1}$  crosses over from  $\propto T^3$  to  $T$  seems to be somewhat below  $T_c$  compared to the experimental result [16], this is mainly because we have taken  $\Delta_0/t_b$  and  $T_c/t_b$  to be larger than in the actual material due to the restriction in the numerical calculations. We have confirmed that this crossover temperature becomes higher for smaller  $\Delta_0$ , so that a more quantitative agreement with the experiment is expected for more realistic values of  $\Delta_0/t_b$ .

Finally, we discuss the pairing symmetry in the actual TMTSF superconductor. The magnetic field is applied along the  $a$  axis in the experiment [16] to remove the effect of the vortices on  $T_1^{-1}$ . However, our results show that the effect of the vortices is not negligible in unconventional superconductors with line nodes and that  $T_1^{-1}$  is proportional to  $T$  at sufficiently low temperatures. When large magnetic field is applied in other directions, the effect of vortices can be even more remarkable. In fact,  $T_1^{-1} \propto T$  was also observed under a magnetic field in the  $b$  direction [29]. In a very weak magnetic field,  $T_1^{-1}$  is considered to be proportional to  $\propto T^3$  as observed in the experiment for  $(\text{TMTSF})_2\text{ClO}_4$  [19]. This further indicates that (i) the gap has line nodes that intersect the Fermi surface and (ii) the  $T$ -linear behavior at high magnetic field is caused by the effect of the vortices. We cannot discriminate between  $d$  and  $f$  waves solely from  $T_1^{-1}$ , but if we combine this with the Knight shift [16] and the  $H_{c2}$  measurement [17], triplet  $f$ -wave pairing seems to be the most promising candidate for the pairing state.

In summary, we have studied the quasiparticle states and the temperature dependence of the nuclear spin relaxation rate  $T_1^{-1}$  in a quasi-one-dimensional organic superconductor  $(\text{TMTSF})_2\text{PF}_6$ . We have considered the situation in which a magnetic field is applied along the chain direction as in the experiment. As for the superconducting state, we have assumed three pairing symmetries ( $p$ ,  $d$ , and  $f$  waves). Although the suppression of the order parameters near the Josephson vortex is very small, the Josephson vortex induces quasiparticles at the Fermi energy when the gap has line nodes ( $d$ - and  $f$ -wave symmetries). As a result, the LDOS at the Fermi energy near the vortex becomes finite in the magnetic field. Since  $T_1^{-1}$  at low temperatures is very sensitive to the LDOS near the Fermi energy,  $T_1^{-1}$  is proportional to  $T$  in  $d$ - and  $f$ -wave symmetries. On the other hand, in the fully gapped case ( $p$ -wave symmetry), no quasiparticles are induced at the Fermi energy even in the magnetic field, so that the exponential dependence of  $T_1^{-1}$  on  $T$  remains unchanged. We conclude that the relation  $T_1^{-1} \propto T$  observed in  $(\text{TMTSF})_2\text{PF}_6$  [16] is evidence for line nodes in the gap. Together with several experimental observation indicating spin-triplet pairing [16,17], our results suggest that the

$f$ -wave symmetry is the most promising candidate for Q1D organic superconductors.

We thank K. Kanoda for useful discussion on the NMR experiment in organic superconductors. This work was supported by a Grant-in-Aid for the 21st Century COE "Topology Science and Technology" at Hokkaido University. K.K. acknowledges support from the Grant-in-Aid for Scientific Research from the Ministry of Education, Culture, Sports, Science and Technology of Japan.

---

\*Current address: Frontier Research System, RIKEN, Saitama 351-0198, Japan.

- [1] K. Bechgaard *et al.*, Solid State Commun. **33**, 1119 (1980).
- [2] D. Jerome *et al.*, J. Phys. (Paris), Lett. **41**, L95 (1980).
- [3] H. Shimahara, J. Phys. Soc. Jpn. **58**, 1735 (1989).
- [4] K. Kuroki and H. Aoki, Phys. Rev. B **60**, 3060 (1999).
- [5] H. Kino and H. Kontani, J. Low Temp. Phys. **117**, 317 (1999).
- [6] R. Duprat and C. Bourbonnais, Eur. Phys. J. B **21**, 219 (2001).
- [7] A. A. Abrikosov, J. Low Temp. Phys. **53**, 359 (1983).
- [8] Y. Hasegawa and H. Fukuyama, J. Phys. Soc. Jpn. **56**, 877 (1987).
- [9] A. G. Lebed, Phys. Rev. B **59**, R721 (1999).
- [10] K. Kuroki *et al.*, Phys. Rev. B **63**, 094509 (2001).
- [11] Y. Fuseya *et al.*, J. Phys. Condens. Matter **14**, L655 (2002).
- [12] J. C. Nickel *et al.*, Phys. Rev. Lett. **95**, 247001 (2005).
- [13] Y. Tanaka and K. Kuroki, Phys. Rev. B **70**, 060502(R) (2004).
- [14] K. Kuroki and Y. Tanaka, J. Phys. Soc. Jpn. **74**, 1694 (2005).
- [15] Y. Fuseya and Y. Suzumura, J. Phys. Soc. Jpn. **74**, 1263 (2005).
- [16] I. J. Lee *et al.*, Phys. Rev. Lett. **88**, 017004 (2002).
- [17] I. J. Lee *et al.*, Phys. Rev. Lett. **78**, 3555 (1997).
- [18] Y. Hasegawa and H. Fukuyama, J. Phys. Soc. Jpn. **56**, 877 (1987).
- [19] M. Takigawa *et al.*, J. Phys. Soc. Jpn. **56**, 873 (1987).
- [20] M. Takigawa *et al.*, Phys. Rev. Lett. **83**, 3057 (1999); J. Phys. Soc. Jpn. **69**, 3943 (2000).
- [21] M. Takigawa *et al.*, Phys. Rev. Lett. **90**, 047001 (2003); J. Phys. Soc. Jpn. **73**, 450 (2004).
- [22] B. G. Silbernagel *et al.*, Phys. Rev. Lett. **17**, 384 (1966).
- [23] K. Ishida *et al.*, Solid State Commun. **90**, 563 (1994); J. Phys. Soc. Jpn. **63**, 1104 (1994).
- [24] J. R. Clem and M. W. Coffey, Phys. Rev. B **42**, 6209 (1990).
- [25] M. Ichioka and T. Tsuneto, J. Low Temp. Phys. **96**, 213 (1994).
- [26] M. Ichioka, Phys. Rev. B **51**, 9423 (1995).
- [27] Y. Tanuma *et al.*, Phys. Rev. B **64**, 214510 (2001).
- [28] M. Takigawa *et al.*, Phys. Rev. B **65**, 014508 (2002).
- [29] I. J. Lee *et al.*, Phys. Rev. B **68**, 092510 (2003).